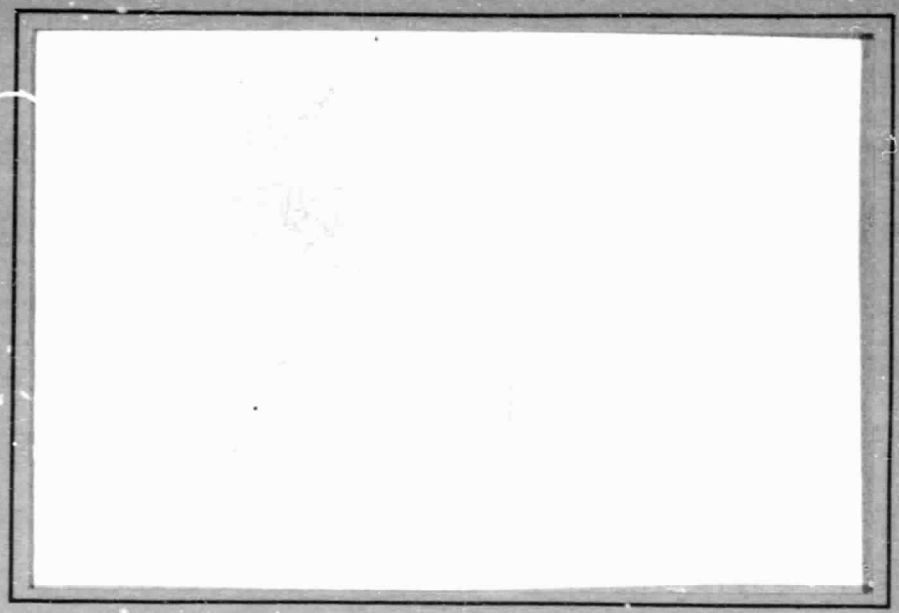

Virginia Polytechnic Institute and State University

Chemistry Department

Blacksburg, Virginia 24061

FINAL TECHNICAL REPORT

AN INVESTIGATION OF ADHESIVE/ADHEREND AND FIBER/MATRIX INTERACTIONS

PART B - SEM/ESCA ANALYSIS OF FRACTURE SURFACES

by

B. Beck, E. Widyani and J. P. Wightman

Prepared for

National Aeronautics and Space Administration

January, 1983

Grant NAG 1-127

NASA-Langley Research Center
Hampton, Virginia 23665
Materials Division
Donald J. Progar

Department of Chemistry
Virginia Polytechnic Institute and State University
Blacksburg, Virginia 24061

FORWARD

This part (Part B) of the final technical report summarizes our research on a fundamental study of adhesion with emphasis on the analysis of fracture surfaces. The results of an extended study of the characterization of titanium, titanium 6-4 and titanium dioxide powders have been reported (1) in Part A.

A listing of papers presented and papers published during the grant period is contained in Appendix.

TABLE OF CONTENTS

LIST OF TABLES

LIST OF FIGURES

GLOSSARY

TECHNIQUES

EDAX - Energy dispersive analysis of x-rays

ESCA - Electron spectroscopy for chemical analysis

SEM - Scanning electron microscopy

OTHERS

A.F. - Atomic fraction

B.E. - Binding energy

LaRC - Langley Research Center

FWT - Flatwise tensile

AFS - Adhesive failure surface

MFS - Metal failure surface

MSS - Metal substrate surface

ABSTRACT

A fundamental study of adhesion has continued with particular emphasis on (i) the characterization of surface oxide layers, (ii) the analysis of fracture surfaces and (iii) the interaction of matrices and fibers. A number of surface features of the fractured lap shear samples were noted in the SEM photomicrographs including the β-phase alloy of the Ti 6-4 adherend, the imprint of the adherend on the adhesive failure surface, increased void density for high temperature samples and the alumina filler particles. Interfacial failure of some of the fractured lap shear samples is invariably characterised by the appearance of an ESCA oxygen photopeak at 530.3 eV assigned to the surface oxide layer of Ti 6-4 adherend. The effect of grit blasting on carbon fiber composites is evident in the SEM analysis. A high surface fluorine concentration on the composite surface is reduced some ten-fold by grit blasting.

I. INTRODUCTION

A long-term, continuing NASA goal is to develop improved adhesives and composite matrices for construction of advanced aircraft and space vehicles. The extreme conditions encountered in these applications demand a unique combination of processability, toughness and durability. One aspect of this multi-faceted program is the development of an autoclaveable, high-temperature adhesive system for joining titanium/titaniumn, titanium/composite, and composite/composite intended to serve structurally for thousands of hours at 505 K (450°F) and hundreds of hours at 589 K (600°F). Another aspect is the development of a toughened (more impact resistant) matrix resin for use in conventional take-off and landing vehicles that require use at 366 K (200°F) for 50,000 hours.

Early work emphasized synthesis and strength-testing of novel high-temperature polyimides, including variations in solvent, amine and anhydride in the adhesive formulation; aluminum, titanium and composite adherends; high-temperature aging and strength-testing; and aluminum powder adhesive filler. The surface characteristics associated with joint strength were evaluated using ESCA, SEM/EDAX, specular reflectance infrared spectroscopy (SRIRS) and contact angles in a variety of experiments (2-7). Based upon these results, SEM/EDAX stood out as most effective because detailed analysis of the surface structures of fractured joints revealed unique characteristics typical of specific adhesive formulations and test conditions.

The total strength of an adhesive joint can be attributed to four factors: inherent flaws, interfacial failure, deformation (elastic and plastic) and fracture (cracking and crazing). "After-the-fact" analysis of fractured adhesive joints with the SEM coupled with ESCA points out what the strength was due to or where the weak link was. Surface analysis of representative samples of a number of NASA-LaRC studies have been reported (8-12) using the combined SEM/EDAX/ESCA techniques.

A major thrust of the present research concerns the characterization of the oxide layer on Ti 6-4. Properties of this oxide layer can have a marked influence on bond strength and on bond durability. "Researchers have observed that the single most critical parameter influencing bond strength and durability of adhesively bonded aluminum structures is the surface preparation of the metal before bonding" (13). The importance of surface preparations is not unique to aluminum, but would be critical for any adherend. The results of several studies (14,15) bespeak the subtle yet dramatic differences in surface structure and composition of titanium alloys pretreated in different ways.

Wegman (16) has shown for aluminum, titanium, and glass resin composite

adherends that the adhesives are less effected by the environment than the adherends. For titanium, it was noted, however, that an increase in humidity decreased the durability of the stress bonded joint. The only effect that temperature had on the durability of the joint was to weaken it initially. On the other hand, bond durability was much improved when the titanium was pretreated with a phosphate/fluoride etch rather than an alkaline etch. This conclusion supports the premise that attention has to be focused on the effect of adherend pretreatment on surface structure and composition.

There has been increased interest (17) in relating surface acidity to observed properties in interfacial systems. For example, Fowkes (18) has argued cogently that maximum adhesive strength should result from a proper matching of the acid-base properties of the adhesive and adherend. Indeed, some of our recent efforts (19) have been directed towards a characterization of the surface acidity of pretreated Ti 6-4. Here, diffuse reflectance visible spectroscopy is used to obtain the spectra of indicator dyes on pretreated Ti 6-4 coupons.

Any fundamental approach to adhesion involves thermydynamic analysis. Contact angle measurements and establishment of the critical surface tension have been widely used in support of interfacial thermodynamics (20). A significant thermodynamic measurement which has not been emphasized and which in fact has been neglected is calorimetry. The Calvet microcalorimeter (21) is uniquely suited to the thermal analysis of adhesion systems due to (i) its high sensitivity and (ii) its long term stability. These are critical considerations since enthalpy changes in polymeric adhesive systems may be small and may occur over extended periods of time.

A broad three phase research effort has been initiated and the objectives are outlined below. The first phase was a detailed characterization of the

oxide layer on Ti 6-4 surfaces by spectroscopic and calorimetric techniques. The second phase was the analysis of Ti 6-4 adherend surfaces after fracture of adhesively bonded samples. The third phase involved an investigation on the interaction of matrix and fiber. Results obtained pursuant to objective (i) have been reported (1). The present report details results obtained pursuant to objectives (ii) and (iii).

II. EXPERIMENTAL

A. Materials

1. Fractured Lap Shear Samples - One hundred and fifty fractured lap shear samples were supplied by personnel at the Boeing Company under NASA Contract NAS1-15605. The particular samples which were analyzed during the current grant period are listed in Table I. The average lap shear strength is listed and also the strength of the particular sample used in our study is given in parenthesis.

2. Flatwise Tensile (FWT) Samples - Two FWT samples coded No. 2-20 and No. 3-26 were analyzed. A description of the samples is given in Table II.

3. Composite Panels - Two LARC 160/Celion 6000 composite panels were analyzed. Panel No. P-1-G #1 was washed and rinsed with methanol and air dried for 30 min at 100°C. Panel No. P-1-G #2 was washed and rinsed with methanol, grit blasted with 120 grit alumina, washed and rinsed with methanol then air dried for 30 min at 100°C.

B. Methods and Procedures

1. Scanning Electron Microscopy/Energy Dispersive Analysis of X-rays (SEM/EDAX) - SEM photomicrographs at various magnifications were obtained on an AMR scanning electron microscope (Advanced Metals Research Corporation Model 900). Approximate vertical dimensions of each photomicrograph appear at the

TABLE I

DESCRIPTION OF BOEING FRACTURED LAP SHEAR SAMPLES

Boeing Designation*	Lap Shear Strength(PSI)
[L13-E-1, RT]	910.
[L13-E-8, 450]	0
[L13-G-3, RT]	1750.
[L13-G-4, 450]	48.
[L13MI-E-7, RT]	1250.
[L13MI-E-4, 450]	1000.
[L13MI-G-9, RT]	2100.
[L13-MI-G-4, 450]	1556.

*Adhesive resin (L13 or L13 MI) - Phosphate/Fluoride Etch: Picatinny Modified (E) or Turco 5578 Alkaline Etch (G) - Sample No. - Test Temperature

TABLE II

DESCRIPTION OF FLATWISE TENSILE SAMPLES

	Sample No.	
Component	2-20	3-26
Adhesive	LARC-13	NR-056X
Primer	LARC-13	NR-056X
Skin Material	LARC-160/Celion-6000	LARC-160/Celion-6000
Honeycomb Core	HRH-327 PI/Glass	HRH-327 PI/Glass

right in the figures, and the corresponding magnif ation is listed in each caption. Most SEM samples were run after ESCA analysis. A thin (~ 20 nm) film of Au-Pd Alloy was vacuum-evaporated onto the samples to enhance conductivity of insulating samples which were mounted on an Al sample stub with copper conductive tape. A rapid semi-quantitative elemental analysis was obtained on selected samples with an EDAX International Model 707A energy-dispersive X-ray fluorescence analyzer attached to the AMR-900 SEM. A photographic record of each EDAX spectrum was made using a camera specially adapted for the EDAX oscilloscope.

2. Electron Spectroscopy for Chemical Analysis (ESCA) - ESCA data were collected on a DuPont 650 photoelectron spectrometer with a magnesium anode ($h\nu$ = 1253.6 ev) and direct display of the spectra on an x-y recorder. The carbon 1s level (taken at 285.0 ev) was used to evaluate the work function of the spectrometer. Circular (6.4 mm diameter) samples were mounted on the copper sample probes using double sided adhesive tape.

III. RESULTS AND DISCUSSION

A. Fractured Lap Shear Samples - L13.

The fractured lap shear samples are discussed by polymer type, pretreatment and strength test temperature. An extensive series of SEM photomicrographs were taken of the samples studied in the present work. It is not the purpose of this report to present and discuss all of these SEM photomicrographs. Rather, the approach has been to point out similarities to what has already been presented. A great deal of material has thus been eliminated without sacrificing an understanding of the results.

The fractured lap shear samples were first examined visually and the

failure classified as (i) interfacial (mostly adhesive showing on one member, mostly metal showing on the other member) (ii) cohesive (adhesive showing on both members) and (iii) mixed mode (significant amounts of metal and adhesive showing on both members). Generally, lower lap shear strehgths were associated with interfacial failure. For some of the interfacial failure samples, the adhesive on one member "popped off" when the sample was punched for ESCA/SEM analysis. Thus four surfaces were generated as depicted in Figure 1.

1. L13-Phosphate/Fluoride Etch: Picatinny Modified - Room Temperature [L13-E-1, RT] - Representative SEM photomicrographs of the metal failure surface (MFS), the adhesive failure surface (AFS) and the metal substrate surface (MSS) for this sample are shown in Figure 2. Features characteristic of Ti 6-4 following a phosphate/fluoride (Picatinny) etch (12) are seen in Figures 2A and 2B for the metal failure surface (MFS). The small white "particles" seen on the surface are in fact the β phase of this alloy.

The imprint of the adherend on the adhesive failure surface (AFS) is clearly seen in the SEM photomicrograph in Figure 2C on comparison with Fig. 2B. In addition, cracks and/or voids are noted on the adhesive failure surface. The nodule in the center of Fig. 2C is an alumina particle based on EDAX analysis. Alumina is a component of the L13 adhesive.

The SEM photomicrograph of the metal substrate surface (MSS) is shown in Figure 2D. Similar features are seen on comparing Fig. 2D with Fig. 2A. Thus, minimal adhesive remains on the metal substrate surface (MSS).

The ESCA results for these samples are listed in Table III. A doublet O 1s photopeak was observed for the metal failure surface (MFS). The photopeak at 531.8 eV is assigned to oxygen in the adhesive whereas the photopeak at 530.6 eV is assigned to oxygen in the titanium oxide surface layer of the adherend. A small Ti photopeak at 458.8 eV is also observed indicating

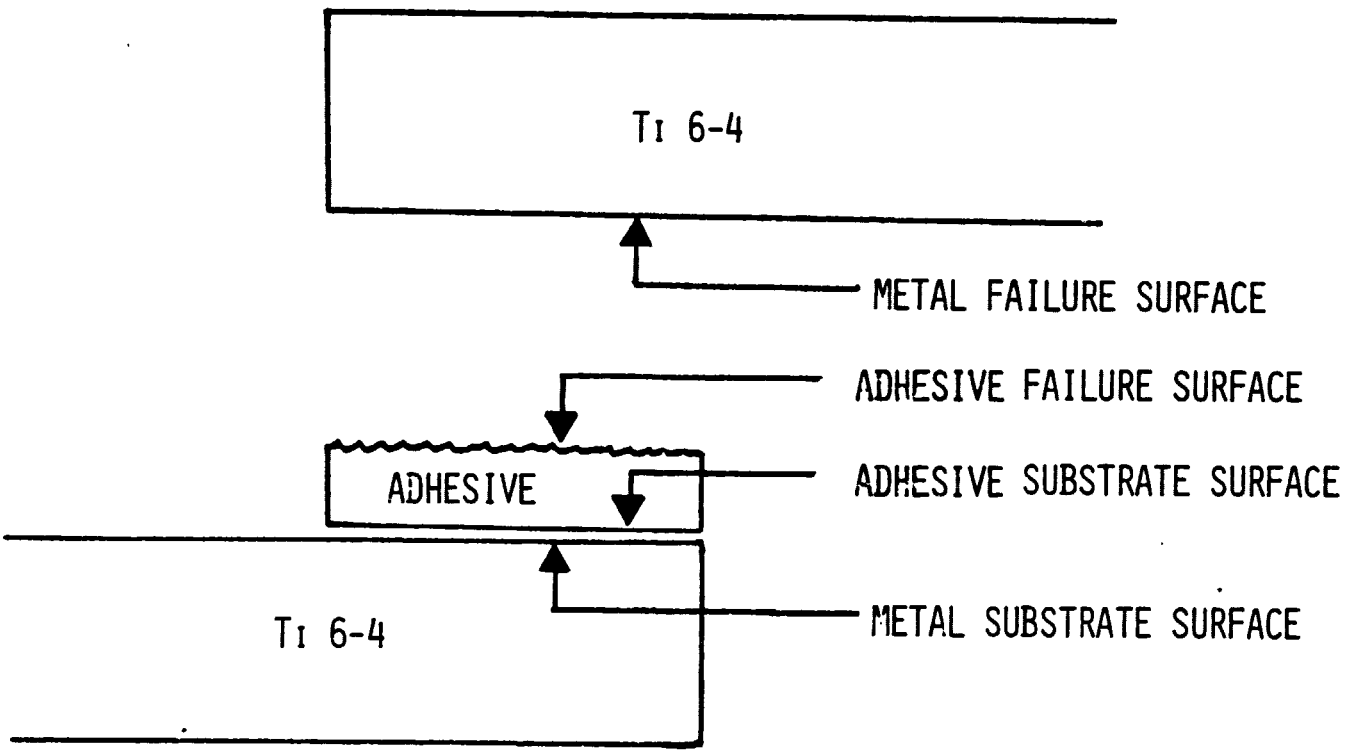

Figure 1. Schematic of fractured lap shear specimen.

Figure 2. SEM photomicrographs of the metal failure surface at 1000X (A); at 5000X (B); of the adhesive failure surface at 5000X (C); of the metal substrate surface at 550X (D) for Sample No. [L13-E-1, RT].

Figure 2. SEM PHOTOMICROGRAPHS FOR SAMPLE NO. [L13-E-1, RT].

(A) METAL FAILURE SURFACE AT 1000X

(B) METAL FAILURE SURFACE AT 5000X

(C) ADHESIVE FAILURE SURFACE AT 5000X

(D) METAL SUBSTRATE SURFACE AT 550X

significant adherend areas with only an ultrathin (< 5 nm) overlayer of adhesive. The carbon photopeak at 288.6 eV is characteristic of carbon contained in carbonyl or carboxylate groups. This photopeak was in fact observed on all but one sample.

The ESCA results in Table III for the adhesive failure surface (AFS) indicate only the presence of oxygen characteristic of the adhesive. The absence of a significant Ti photopeak is taken as evidence for interfacial failure between the adherend and the surface oxide layer.

The metal substrate surface (MSS) gives again an oxygen doublet showing that both adhesive and adherend surface oxide are on this sample. It is emphasized that this level of atomic definition is possible with the ESCA technique but not with the SEM technique.

2. L13-Phosphate/Fluoride Etch: Picatinny Modified - 450° [L13-E-8, 450] - The SEM photomicrographs of the metal failure surface (MFS) and metal substrate surface (MSS) for this sample were similar to those for the [L13-E-8, RT] sample discussed above in Section 1. Thermal treatment of the lap shear sample at 450°F did not alter surface features of either the metal failure surface or the metal substrate surface. On the other hand, some differences were noted in the SEM photomicrograph of the adhesive failure surface (AFS) shown in Figure 3A. This surface contained a greater density of voids perhaps due to the higher temperature compared to the room temperature sample.

The ESCA results for the metal failure surface (MFS) are listed in Table III. Again, the oxygen doublet photopeak and the titanium photopeak are indicative of a minimal adhesion overlayer and thus failure for this sample can be assigned as interfacial between the adhesive and the adherend surface oxides. The adhesive failure surface (AFS) gives only a single oxygen photopeak. In addition, a small silicon photopeak is observed perhaps due to

Figure 3. SEM photomicrographs of the adhesive failure surface at 50X (A) for Sample No. [L13-E-8, RT]; of the metal failure surface at 500X (B) for Sample No. [L13-G-3, RT]; of the adhesive failure surface at 100X (C) for Sample No. [L13-G-4, 450]; of the adhesive failure surface at 100X (D) for Sample No. [L13MI-G-4, 450].

Figure 3. SEM PHOTOMICROGRAPHS OF THE

(A) ADHESIVE FAILURE SURFACE AT 50X FOR SAMPLE NO. [L13-E-8, RT]

(B) METAL FAIURE SURFACE AT 500X FOR SAMPLE NO. [L13-G-3, RT]

(C) ADHESIVE FAILURE SURFACE AT 100X FOR SAMPLE NO. [L13-G-4, 450]

(D) ADHESIVE FAILURE SURFACE AT 100X FOR SAMPLE NO. [L13MI-G-4, 450]

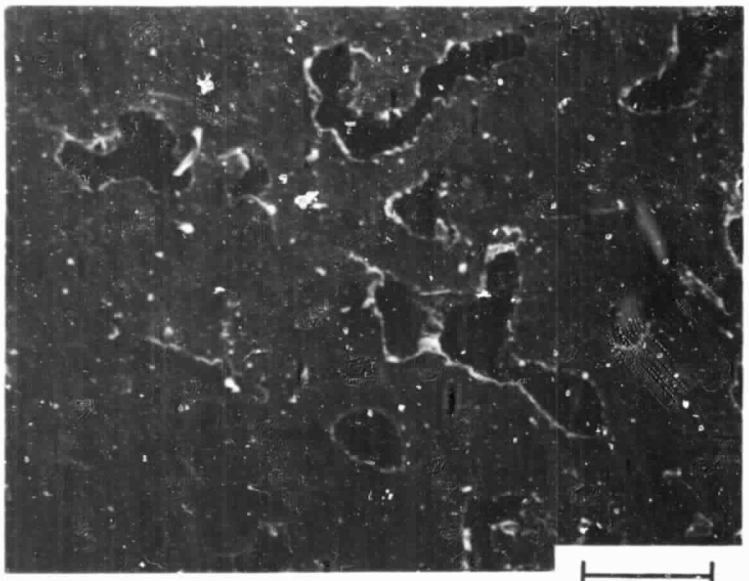

A

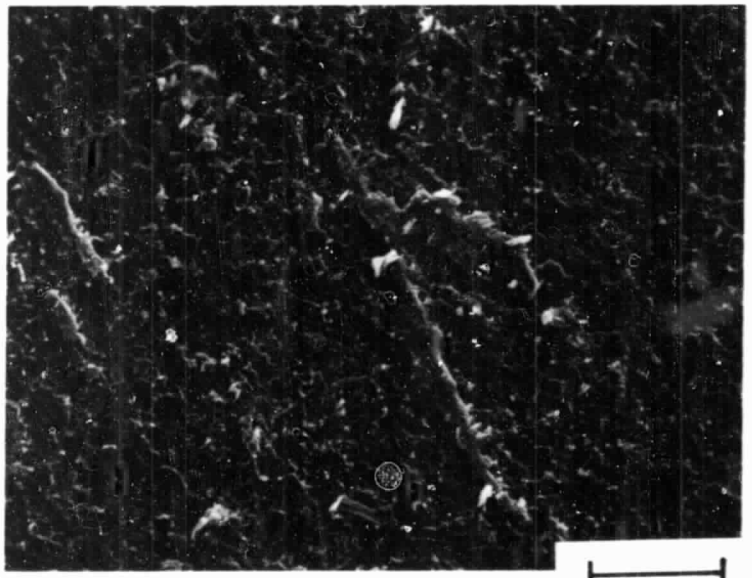

B

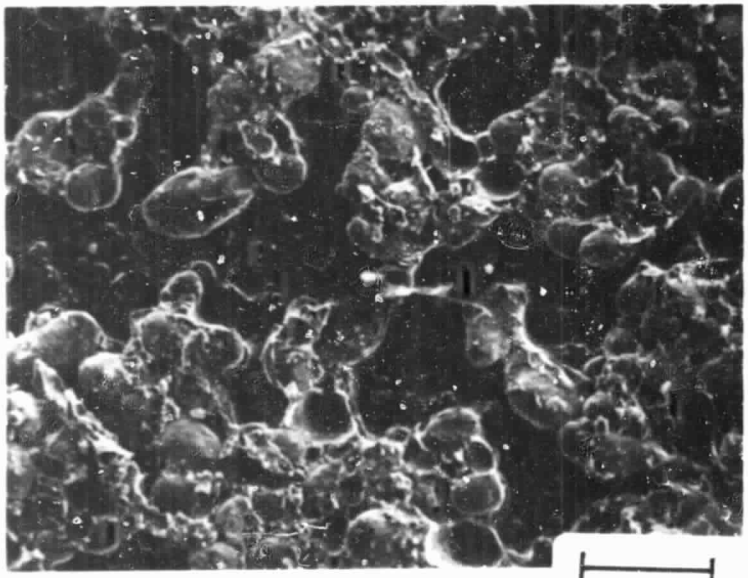

C

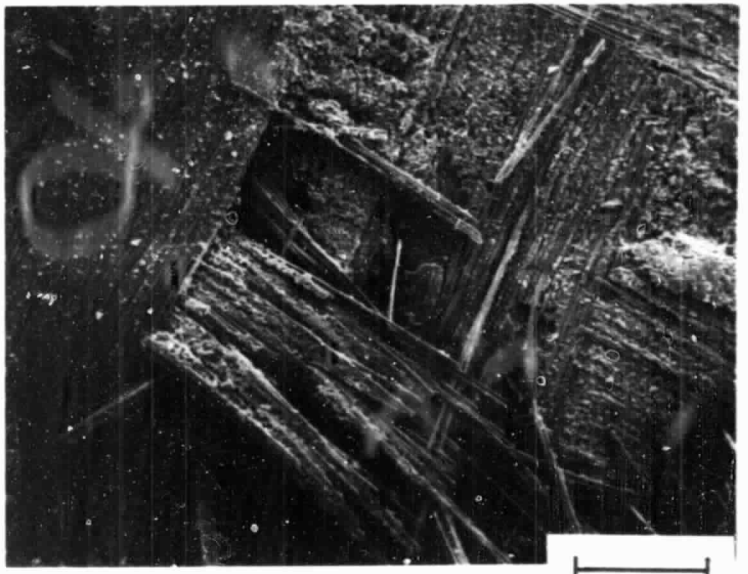

D

TABLE III

ESCA RESULTS OF FRACTURED LAP SHEAR SAMPLES - L13

Sample No.	Surface Analyzed	Photopeak	B.E.(eV)	A.F.
L13-E-1,RT	AFS	O 1S	532.2	0.12
		N 1s	400.5	0.043
		C 1s	288.4	
			285.0	0.83
	MFS	O 1s	531.8	
			530.6	0.28
		Ti 2p3	458.8	0.050
		N 1s	400.7	0.021
		C 1s	288.6	
			285.0	0.65
	MSS	O 1s	531.7	
			530.4	0.29
		Ti 2p3	458.7	0.058
		N 1s	400.5	0.023
		C 1s	288.6	
			285.0	0.63
L13-E-8, 450	AFS	O 1s	532.0	0.14
		N 1s	400.3	0.033
		C 1s	288.2	
			285.0	0.81
		Si 2p	102.4	0.022
	MFS	O 1s	531.7	
			530.0	0.27
		Ti 2p3	458.5	0.042
		N 1s	400.0	0.025
		C 1s	288.3	
			285.0	0.66
	MSS	O 1s	531.8	
			530.3	0.26
		Ti 2p3	458.7	0.057
		N 1s	400.6	0.023
		Ca 2p3	347.4	0.007
		C 1s	288.5	
			285.0	0.65

TABLE III CONTINUED

Sample No.	Surface Analyzed	Photopeak	B.E.(eV)	A.F.
L13-G-3, RT	-	O 1s	532.2	
			530.2	0.26
		Ti 2p3	458.6	0.035
		N 1s	400.4	0.028
		C 1s	288.4	
			285.0	0.67
L13-G-4, 450	-	O 1s	532.1	0.20
		Ti 2p3	-	NSP
		N 1s	400.2	0.034
		C 1s	285.0	0.68
		Al 2p	120.3	0.093

the scrim cloth used in bonding. The metal substrate surface (MSS) yields again an oxygen doublet with a titanium photopeak but also a calcium photopeak at 347.4 eV. We have reported previously (12) calcium as a trace element on Ti 6-4 following phosphate/fluoride etch.

3. L13 - Turco 5578 Alkaline Etch - Room Temperature [L13-G-3, RT] - The SEM photomicrograph of the metal failure surface (MFS) for this sample is shown in Figure 3B. A high density of β-phase "flakes" results from the Turco pretreatment of Ti 6-4 (12). Although, some of these "flakes" are shown circled in Fig. 3B, the surface also appears to have on it a fair amount of residual adhesive. The ESCA results listed in Table III support the conclusion of a fair amount of exposed adherend band on the oxygen photopeak at 530.2 eV and the titanium photopeak at 458.6 eV.

4. L13 - Turco 5578 Alkaline Etch - 450° [L13-G-4, 450] - An SEM photomicrograph of the adhesive failure surface (AFS) of this sample is shown in Figure 3C. Here regions of the adhesive with alumina particles showing (and missing) and void areas are noted. The alumina particles were not "pulled out" following fracture at room temperature whereas this was the case at 450°F. The ESCA results in Table III support the assignment of exposed alumina as deduced from the photopeak at 120.3 eV. No titanium is noted on this surface suggesting failure in the adhesive but close to the adherend surface oxide layer.

B. Fractured Lap Shear Samples - L13 MOD I

1. L13MI - Phosphate/Fluoride Etch: Picatinny Modified - Room Temperature [L13MI-E-7, RT] -SEM photomicrographs of the adhesive failure surface (AFS) of this sample showed quite similar features to those noted in Fig. 2C. There were no discernable features to differentiate between the L13

and L13MI adhesives. Only photopeaks characteristic of the adhesive were observed for this sample as listed in Table IV.

2. L13MI - Phosphate/Fluoride Etch: Picatinny Modified - 450° [L13MI-E-4, 450] - SEM photomicrographs of the adhesive failure surface (AFS) of this sample showed similar features to those noted in Fig. 3B. Again, no differentiation was possible based on the SEM work on the L13 and L13MI adhesives. Indeed the ESCA results in Table IV were similar for both the L13 and L13MI adhesives on a phosphate/fluoride pretreated Ti 6-4 adherend and tested either at room temperature or 450°F. Specifically, the same major photopeaks were observed for Sample Nos. [L13-E-RT], [L13-E-450], [L13MI-E-RT] and [L13MI-E-450].

3. L13MI - Turco 5579 Alkaline Etch - Room Temperature [L13MI-G-9, RT] - The SEM photomicrographs of the adhesive failure surface (AFS) of this sample showed large areas of fractured scrim cloth. This is in contrast to the microscopy analysis of the L13 sample. A titanium photopeak was observed for this sample (see Table IV) attributed to a small area of exposed adherend. The fact that a major oxygen photopeak was not observed at about 530 eV is additional evidence that the area of exposed adherend is small.

4. L13MI - Turco 5579 Alkaline Etch - 450° [L13MI-G-4, 450] - Significantly a considerable amount of fractured scrim cloth was noted on the adhesive failure side of this sample (see Fig. 3D) as in the preceding one. This suggest that there is a difference between the L13 and L13MI adhesive systems on a Turco pretreated Ti 6-4 surfaces independent of temperature. This was not the case for a phosphate/fluoride pretrested Ti 6-4 surface. Mason, Siriwardane and Wightman (19) have shown that an acidic Ti 6-4 surface results from a phosphate/fluoride pretreatment whereas a basic Ti 6-4 surface results from a Turco pretreatment.

TABLE IV

ESCA RESULTS OF FRACTURED LAP SHEAR SAMPLES - L13MI

Sample No.	Surface Analyzed	Photopeak	B.E.(eV)	A.F.
L13MI-E-7, RT		O 1s	532.1	0.19
		Ti 2p3		NSP
		N 1s	400.2	0.037
		C 1s	288.1	
			285.0	0.77
L13MI-E-4, 450		O 1s	532.0	0.14
		Ti 2p3		NSP
		N 1s	400.3	0.059
		C 1s	288.1	
			285.0	0.80
L13MI-G-9, RT		O 1s	532.1	0.20
		Ti 2p3	459.0	0.012
		N 1s	400.4	0.053
		C 1s	288.3	
			285.0	0.73
L13MI-G-4, 450		O 1s	532.2	0.20
		Ti 2p3		NSP
		N 1s	400.2	0.047
		C 1s	288.0	
			285.0	0.75

The ESCA results in Table IV for this sample shows only a single oxygen photopeak and no significant Ti photopeak.

C. LARC-160/Celion 6000 Composite Panels

Scanning electron microscopy/electron spectroscopy for chemical analysis (SEM/ESCA) techniques have been applied to the analysis of two LARC-160/ Celion 6000 composite panels. SEM analysis of the untreated panel (P-1-G #1) showed a regular array of well-coated fibers as noted in Figure 4A. Carbon, fluorine, nitrogen and oxygen were the elements present in the composite surface as detected by ESCA. The fluorine to nitrogen ratio of 6.3 for this surface was quite high. Evidently, fluorine contamination occurred during fabrication. The grit blasted panel (P-1-G #2) showed extensive changes in surface morphology as noted in Figure 4B. The F/N ratio calculated from the ESCA results also decreased by more than a factor of 10 for the grit blasted panel.

D. Flatwise Tensile Samples

1. Sample No. 2-20 - The side of the LARC 160/Celion 6000 panel adjacent to the honeycomb structure showed similar SEM features to P-1-6 #1 but a number of cracks were noted in the matrix as seen in Figure 4C. The ESCA F/N ratio of 0.55 was similar to the ratio for the grit blasted panel (P-1-G #2).

2. Sample No. 3-26 - This sample yielded 3 surfaces for analysis. The honeycomb structure was examined by SEM and showed fibers well wet by the matrix as can be noted in Figures 5A and 5B. No ESCA analysis was made on this surface because of sample configuration. The surface of the adhesive next to the honeycomb structure and next to the composite panel were analyzed. The SEM photomicrographs were quite different. For example, the honeycomb side (see Fig. 5C) showed no fibers whereas fibers were seen on the composite sides (see Fig. 5D). Again carbon, fluorine, nitrogen and oxygen ESCA

Figure 4. SEM photomicrographs at 500X (A) for Sample No. P-1-G #1; at 500X (B) for Sample No. P-1-G #2; at 500X (C) for the side of FWT Sample No. 2-20 adjacent to the honeycomb structure.

Figure 4. SEM PHOTOMICROGRAPHS OF

(A) SAMPLE NO. P-1-6 #1 at 500X

(B) SAMPLE NO. P-1-6 #2 at 500X

(C) FWT SAMPLE NO. 2-20: SIDE ADJACENT TO HONEYCOMB STRUCTURE.

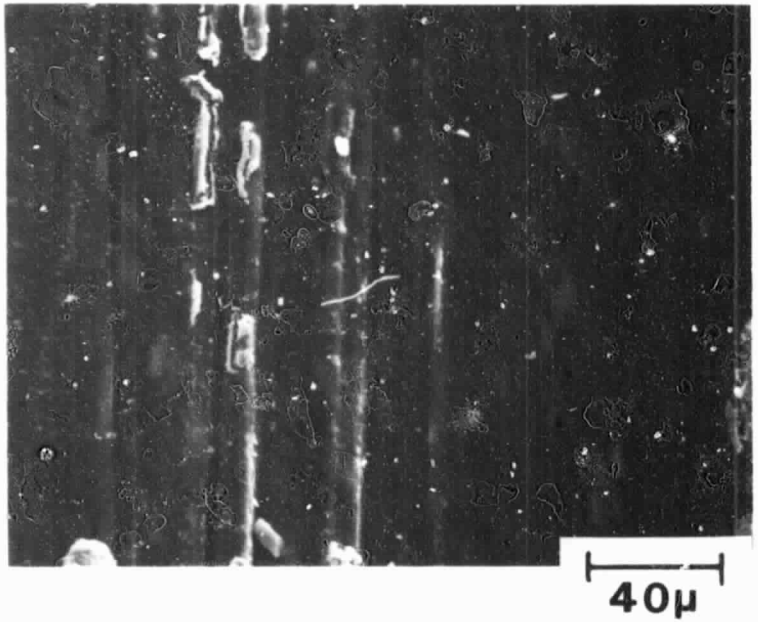

A

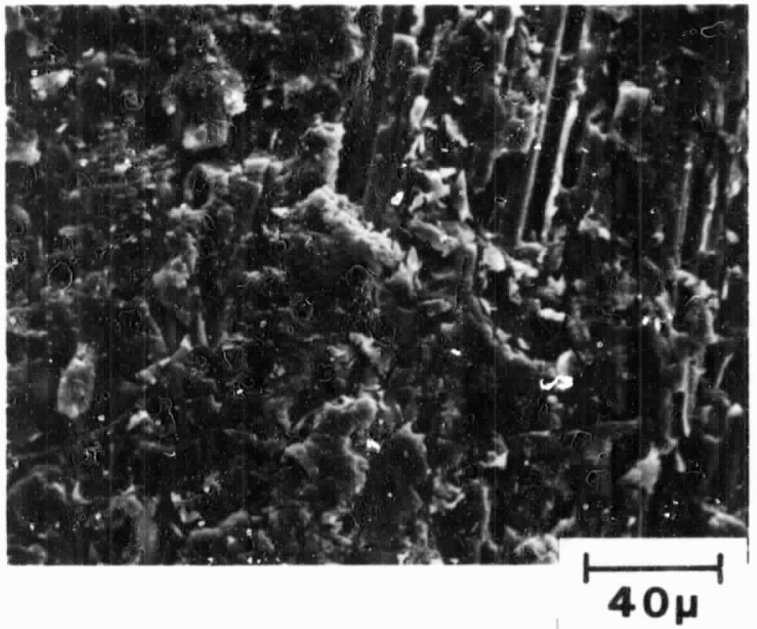

B

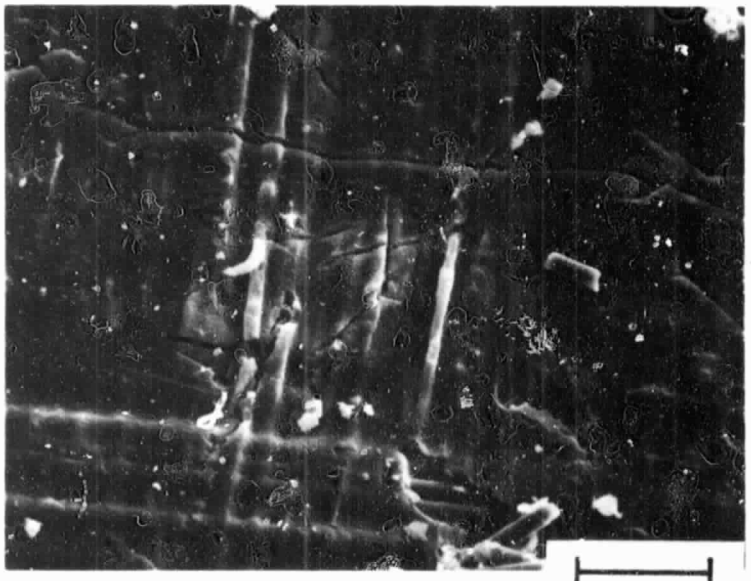

C

Figure 5. SEM photomicrographs at 50X (A) at 500X (B) of the honeycomb structure from FWT Sample No. 3-26; at 500X (C) for the adhesive adjacent to the honeycomb structure; at 500X (D) for the adhesive adjacent to the composite panel.

Figure 5. SEM PHOTOMICROGRAPHS FOR SAMPLE NO. 3-26

(A) HONEYCOMB STRUCTURE AT 50X

(B) HONEYCOMB STRUCTURE AT 500X

(C) ADHESIVE ADJACENT TO HONEYCOMB STRUCTURE AT 500X

(D) ADHESIVE ADJACENT TO COMPOSITE PANEL AT 500X

A

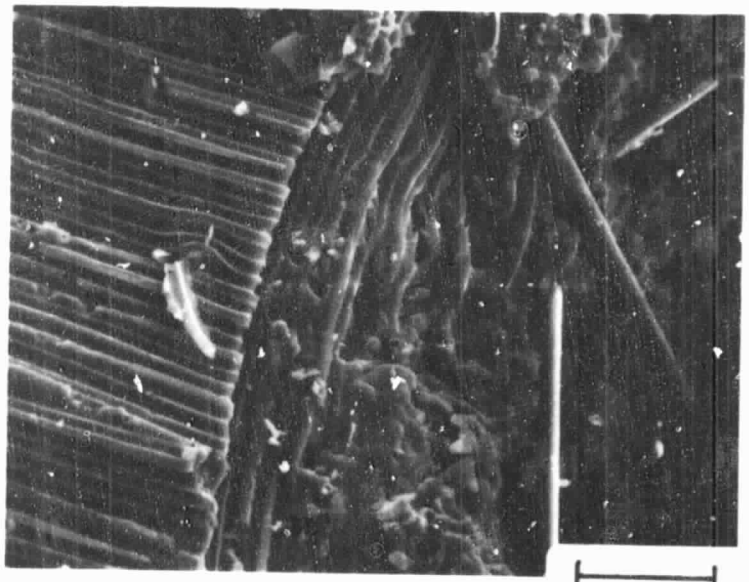

B

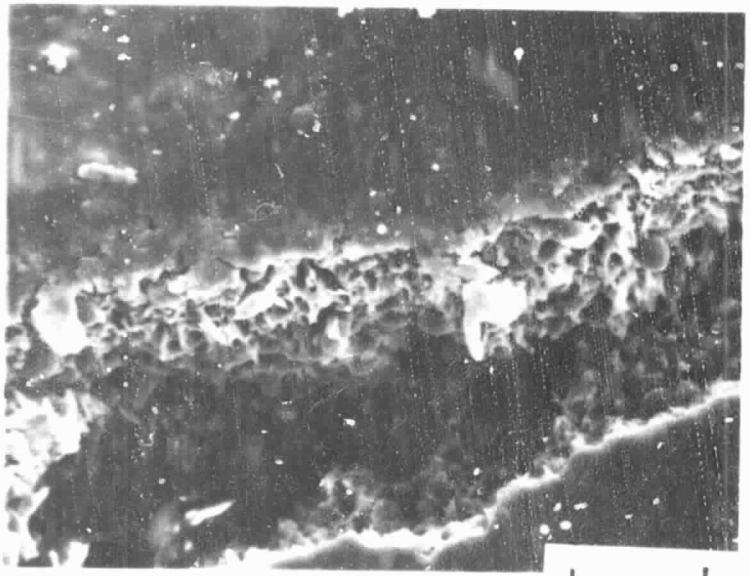

C

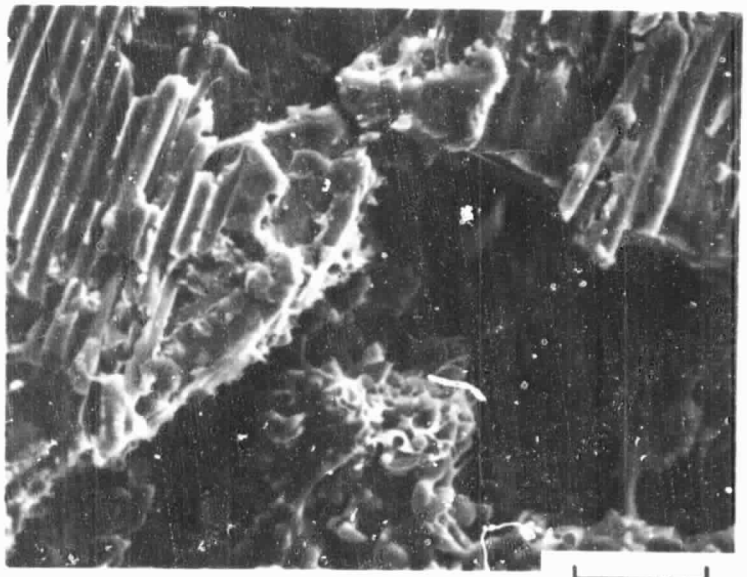

D

photopeaks were observed on both surfaces. The F/N ratio was 2.8 for both samples. The presence of fluorine in this sample is expected since the NR056X adhesive contains fluorine.

IV. REFERENCES

1. R. V.Siriwardane and J. P. Wightman, "An Investigation of Adhesive/Adherend and Fiber/Matrix Interactions. Part A - Surface Characterization of Titanium Dioxide, Titanium and Titanium 6% Al - 4% V Powders: Interaction with Water, Hydrogen Chloride and Polymers". NASA Report NAG1-127, May, 1982.
2. T. A. Bush, M. S. Thesis, Virginia Polytechnic Institute and State University, 1973.
3. T. A. Bush, M. E. Counts, T. C. Ward, J. P. Wightman, "Effect of Polymer Properties and Adherend Surfaces on Adhesion," NASA Contract Report NAS1-10646-14. November, 1973.
4. M. E. Counts and J. P. Wightman, "Effect of Adherend Surfaces on Adhesion," NASA Contract Report-NAS1-10646-25, November, 1974.
5. Thurman A. Bush, Mary Ellen Counts and J. P. Wightman, in Adhesion Science and Technology, Part A, L.-H. Lee, Editor, p. 365, Plenum Press,
6. D. W. Dwight, M. E. Counts, and J. P. Wightman, "Effect of Polymer Properties and Adherend Surfaces on Adhesion," NASA Report NSG-1124, December, 1975.
7. D. W. Dwight, M. E. Counts and J. P. Wightman, in Colloid and Interface Science, Vol. III., M. Kerker, Ed., p. 143, Academic Press, New York (1976).
8. D. W. Dwight and J. P. Wightman, "Effect of Polymer Properties and Adherend Surfaces on Adhesion," NASA Report NSG-1124, February, 1977.

9. D. W. Dwight and J. P. Wightman, "A Fundamental Approach to Adhesion: Synthesis, Surface Analysis, Thermodynamics and Mechanics," NASA Report NSG-1124, February, 1978.

10. W. Chen and James P. Wightman, "A Fundamental Aproach to Adhesion: Synthesis, Surface Analysis, Thermodynamics and Mechanics", NASA Report NSG-1124, January 1979.

11. R. Siriwardane and James P. Wightman, "A Fundamental Approach to Adhesion: Synthesis, Surface Analysis, Thermodynamics and Mechanics, NASA Report NSG-1124, March, 1980.

12. B. Beck, R. Siriwardane and J. P. Wightman, "A Fundamental Approach to Adhesion: Synthesis, Surface Analysis, Thermodynamics", NASA Report NSG-1124, April, 1981.

13. N. T. McDevitt et al., "Surface Studies of Anodic Aluminum Oxide Layers Formed in Phosphoric Acid Solutions," Air Force Materials Laboratory Technical Report, AFML-TR-77-55, May, 1977.

14. G. W. Lively, "Improved Surface Treatments of Titanium Alloys for Adhesive Bonding," Air Force Materials Laboratory Technical Report, AFML-TR-73-270, January, 1974.

15. W. L. Baun and N. T. McDevitt, "Surface Characterization of Titanium and Titanium Alloys. II. Effect on Ti-6Al-4V Alloy of Laboratory Chemical Treatments," Air Force Materials Laboratory Technical Report, AFML-TR-76-29, May, 1976.

16. R. F. Wegman, Appld. Polymer Symp., No. 19, 385-394 (1972).

17. P. Sorensen, J. Paint Technol., 47, 31 (1975).

18. M. J. Marmo, M. A. Mosttafa, H. Jinnai, F. M. Fowkes and J. A. Manson, Ind. Eng. Chem. Prod. Res. Dev., 15, 206 (1976).

19. J. G. Mason, R. Siriwardane and J. P. Wightman, J. Adhesion, 11, 315 (1981).

20. W. A. Zisman, "Advances in Chemistry Series #43, R. F. Gould, Ed. p. 1., Am. Chem. Soc., Washington, DC (1964).

21. E. Calvet and H. Prat, "Recent Progress in Microcalorimetry," Pergamon Press, Oxford (1963).

APPENDIX

LISTING OF PRESENTATIONS AND PUBLICATIONS

Papers Presented

(1) R. Siriwardane and J. P. Wightman, "Surface Characterization of Anatase and Rutile Titanium Dioxide Powders", 55th Colloid and Surface Science Symposium, Cleveland, OH, June, 1981.

(2) B. Beck, W. Chen, R. Siriwardane and J. P. Wightman, "The Application of Spectroscopic Techniques to Metal/Polymer Adhesion", 4th International Conference on Surface and Colloid Science, Jerusalem, Israel, July, 1981.

Papers Published

(1) J. G. Mason, R. Siriwardane and J. P. Wightman, "Spectroscopic Characterization of Acidity of Titanium (6%, Al - 4%, V) Surfaces", J. Adhesion, 11, 315-378 (1981).

(2) J. P. Wightman, "The Application of Surface Analysis to Polymer/Metal Adhesion", SAMPE Quarterly, 13, 1-8 (1981).